

1 Switchable stimulated Raman scattering microscopy with photochromic
2 vibrational probes

3 Jianpeng Ao^{1,‡}, Xiaofeng Fang^{2,‡}, Xianchong Miao¹, Jiwei Ling¹, Hyunchul Kang³,
4 Sungnam Park³, Changfeng Wu^{2*}, and Minbiao Ji^{1*}

5 ¹*State Key Laboratory of Surface Physics and Department of Physics, Human Phenome*
6 *Institute, Multiscale Research Institute of Complex Systems, Academy for Engineering*
7 *and Technology, Key Laboratory of Micro and Nano Photonic Structures (Ministry of*
8 *Education), Fudan University, Shanghai 200433, China*

9 ²*Department of Biomedical Engineering, Southern University of Science and*
10 *Technology, Shenzhen 518055, China*

11 ³*Department of Chemistry and Research Institute for Natural Science, Korea*
12 *University, Seoul, 02841, Korea*

13 [‡] *These authors contributed equally.*

14 ^{*}Corresponding authors: minbiaoj@fudan.edu.cn, wucf@sustech.edu.cn

15

16 **Supplementary Information**

17

18 **Supplementary note 1 – synthesis of DTE-Alkyne derivatives.**

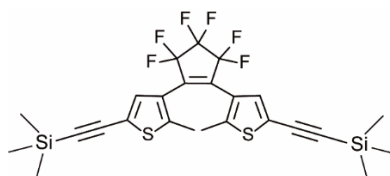
19 **Materials**

20 Tetrahydrofuran (THF), dichloromethane (DCM) methanol, acetone, acetonitrile,
21 acetic acid, triethylamine (Et₃N), sodium hydroxide, and diethyl ether were purchased
22 from Beijing Chemical Plant. Sodium hexafluorophosphate, iodobenzene, Pd(PPh₃)₄,
23 trimethylsilylacetylene, n-BuLi (2.5 M, Hexane solution), perfluorocyclopentene,
24 copper(I) iodide, iodoethane, and 4-(4-iodophenyl)pyridine were purchased from J&K
25 Chemical Ltd. (Beijing, China). Poly (styrene-comaleic anhydride) (PSMA, cumene
26 terminated, average MW \approx 1700, styrene content 68%), N-bromosuccinimide,
27 CD₃OD, and CDCl₃ were purchased from Sigma-aldrich. All the above chemicals were
28 of analytical grade and used as received without further purification. THF was distilled
29 in the presence of sodium benzophenone under protection of dry nitrogen prior to use.

30 **Instruments**

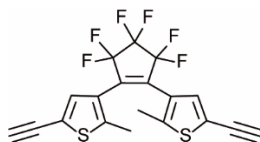
31 ¹H NMR spectra were recorded on a Bruker Avance 400 MHz spectrometer using
32 CDCl₃ or DMSO-d₆ as solvent and tetramethylsilane as an internal standard (d= 0.00
33 ppm). UV-Vis spectra were measured on a Shimadzu UV-2550 spectrophotometer.

34 **Synthesis**



35 **DTE-TMS**

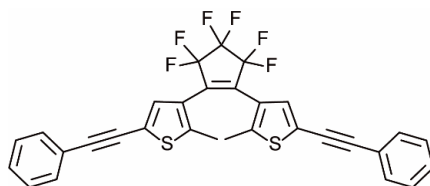
36 The synthesis of all compounds is according to literatures 1-3. ¹H NMR (400 MHz,
37 CDCl₃) δ 7.20 (s, 2H), 1.87 (s, 6H), 0.25 (s, 18H). MS: m/z calcd 560.01; found, 559.01.



DTE-alkyne

38

39 DTE-TMS (1 eq, 0.79 g) was dissolved into methanol/THF (4:1, v:v) mixture under
40 stirring. Then, NaOH (10 eq, 0.6 g) was added and the mixture was stirred at room
41 temperature for 12 h. The resulting mixture was extracted with DCM for three times.
42 The combined organic layer was washed by water, and dried with anhydrous Na₂SO₄.
43 The solvent was evaporated under reduced pressure. The crude product was simply
44 purified by column chromatography over silica gel with hexane as the eluent to yield a
45 white solid (0.39 g, yield: 66.7%). ¹H NMR (400 MHz, CDCl₃) δ 7.23 (s, 2H), 3.36 (s,
46 2H), 1.90 (s, 6H). MS: m/z calcd 416.01; found, 415.01.

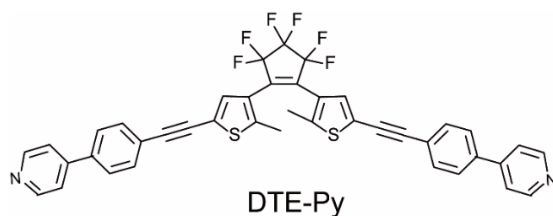


DTE-Ph

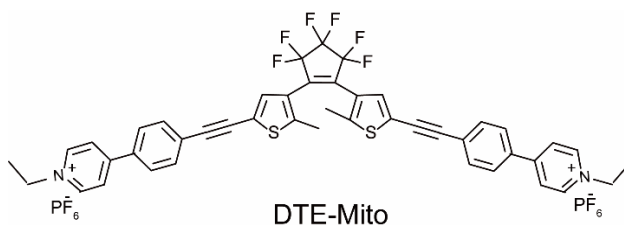
47

48 DTE-alkyne (1 eq, 89.6 mg) and iodobenzene (3 eq, 0.1 mL) were dissolved in 50 mL
49 Et₃N and THF mixture (1:1, v:v). The mixture was degassed by Ar for 30 min,
50 Pd(PPh₃)₄ (5 mg) and copper(I) iodide (2 mg) were added. The reaction mixture was
51 stirred at 70°C for 12 h under Ar atmosphere. After cooling to room temperature, the
52 solvent was evaporated under reduced pressure. The residue was extracted with DCM.
53 The organic layer was washed with HCl (1 M) and water, and then dried over anhydrous
54 Na₂SO₄. The solvent was evaporated under reduced pressure. The crude product was
55 simply purified by column chromatography over silica gel with hexane as the eluent to

56 yield a white solid (92.5 mg, yield: 75.7%). $^1\text{H NMR}$ (400 MHz, CDCl_3) δ 7.51 (dd, J
57 = 6.4, 3.0 Hz, 4H), 7.37 – 7.33 (m, 6H), 7.26 – 7.24 (m, 2H), 1.95 (s, 6H). MS: m/z
58 calcd 568.08; found, 567.07.



59
60 The synthesis of DTE-Py is the same to the DTE-Ph. DTE-alkyne (1 eq, 80 mg) and 4-
61 (4-iodophenyl) pyridine (3 eq, 133 mg) were used. The crude product was simply
62 purified by column chromatography over silica gel with methanol/DCM mixture (1:120,
63 v:v) as the eluent to yield a black green solid (62 mg, yield: 44.5%). $^1\text{H NMR}$ (400
64 MHz, CDCl_3) δ 8.12 – 7.38 (m, 16H), 7.32 (s, 2H), 1.98 (s, 6H). MS: m/z calcd 722.12;
65 found, 723.14.



66
67 DTE-Py (1 eq, 38.4 mg) was dissolved into a 50 mL two-necked round bottom flask
68 with 10 mL acetonitrile. Iodoethane (5 eq, 0.02 mL) was added and the mixture was
69 heated to 80°C for overnight. After cooling to room temperature, 20 mL diethyl ether
70 was added. The black green solids were filtered and washed with diethyl ether. The
71 solids were dissolved in 5 mL methanol/acetone mixture (1:5, v:v) and mixed with
72 saturated NaPF_6 solution (5 mL). After stirring for 1 h, solvent was evaporated. The
73 solids were filtered off again, washed by water and dried under vacuum at 60°C for 24

74 h to yield a black green solid (43.7 mg, yield: 76.9%). ¹H NMR (400 MHz, CD₃OD) δ
75 8.97 (d, J = 6.9 Hz, 4H), 8.42 (d, J = 6.9 Hz, 4H), 8.05 (d, J = 8.5 Hz, 4H), 7.77 (d, J =
76 8.5 Hz, 4H), 7.40 (s, 2H), 4.67 (d, J = 7.4 Hz, 4H), 2.02 (s, 6H), 1.68 (t, J = 7.4 Hz, 6H).
77 MS: m/z calcd 780.21; found, 390.10.

78

79 **Supplementary note 2 – Photo-cyclization conversion ratio measurement.**

80 The area of spontaneous Raman peak is proportional to the content of substance⁴.
81 Therefore, the conversion efficiency of the DTE-Ph is estimated from the Raman
82 spectra intensity variation.

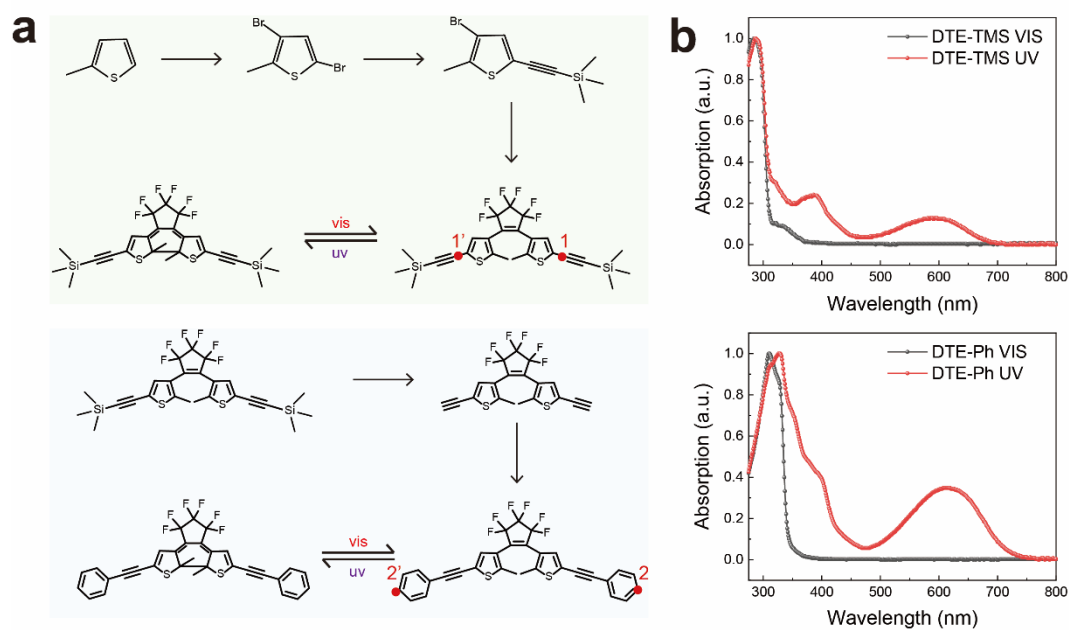
$$83 \quad \phi_{con} = \frac{\int \Delta I dk}{\int I dk}$$

84 Where ϕ_{con} is the conversion efficiency, ΔI is the intensity variation from open-form
85 to closed-form and I is the original intensity of open-form at a certain wavenumber,
86 dk is the wavenumber interval.

87 The conversion efficiency estimation in SRS is more complication due to the lower
88 spectral resolution, so that we need to decompose the SRS spectra. First, the Voigt
89 fitting of the spectrum of layer1 without UV irradiation (Fig. 2a-b, Supplementary Fig.
90 8) gave us the peak position and peak width parameter of open-form. Second, through
91 two Voigt fitting of layer4 while fixing the parameter of open-form, we can derive the
92 peak position and peak width parameter of closed-form. Third, fitting the spectra of all
93 layers with derived parameter, we can calculate each composition percentage
94 (Supplementary Table 1). We can also derive the ratio of SRS intensity of closed-form
95 to open-form and the results from all layers match well.

96

97 **Supplementary Figures**



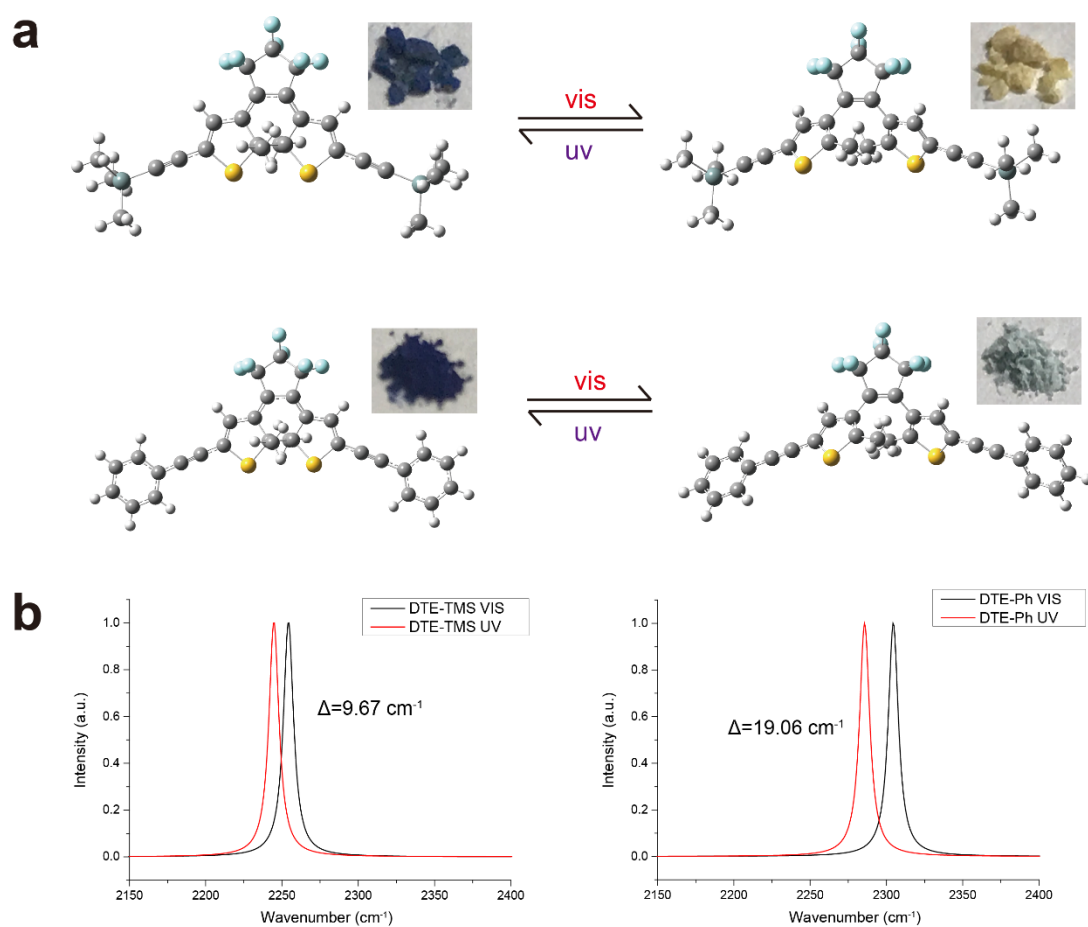
98

99 **Supplementary Fig. 1.** Photo-switching properties of DTE-TMS and DTE-Ph. (a) The

100 synthesis route of DTE-TMS and DTE-Ph; (b) Absorption spectra of DTE-TMS and

101 DTE-Ph after visible or UV irradiation.

102



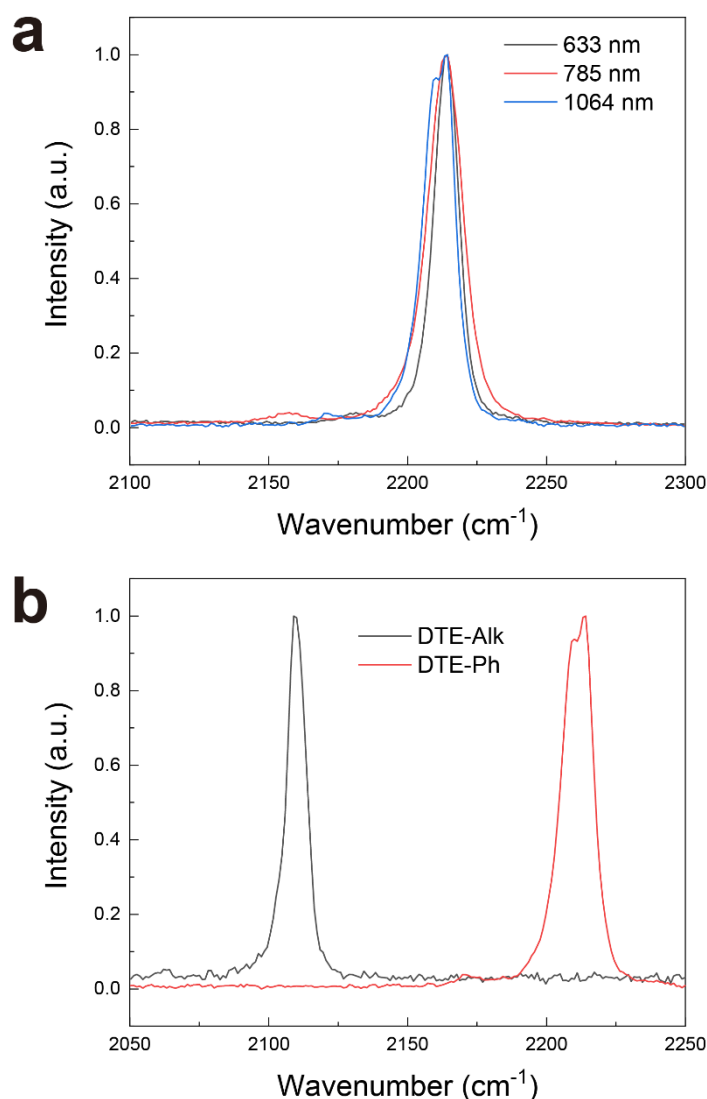
103

104 **Supplementary Fig. 2.** DFT calculation results of DTE-TMS and DTE-Ph. (a) 3D

105 structure and (b) Raman frequency of DTE-TMS and DTE-Ph calculated by Gaussian

106 under B3LYP functional / 6-31g(d) basis set.

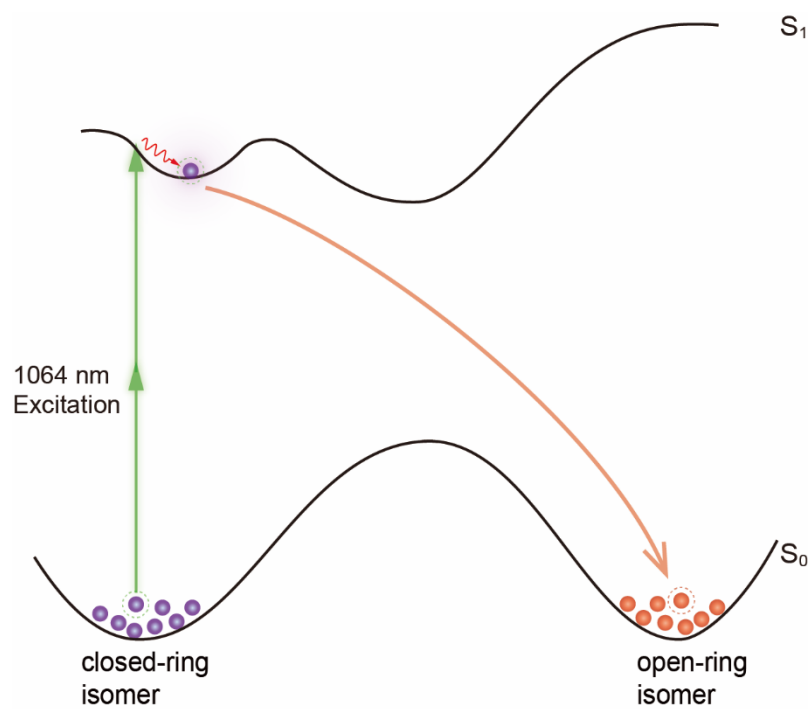
107



108

109 **Supplementary Fig. 3.** Spontaneous Raman spectra of DTE-Ph. (a) Spontaneous
 110 Raman spectra of DTE-Ph measured with 633nm (FWHM ~ 9 cm⁻¹), 785nm (FWHM
 111 ~ 13 cm⁻¹) and 1040nm (FWHM ~ 7 cm⁻¹ for each peak) excitation. (b) Verification of
 112 the small “splitting” appeared in 1064 nm pumped Raman spectroscopy. The DTE-Alk
 113 molecule doesn't show any spectral splitting (FWHM ~ 7 cm⁻¹), excluding systematic
 114 error of the Raman spectrometer.

115



116

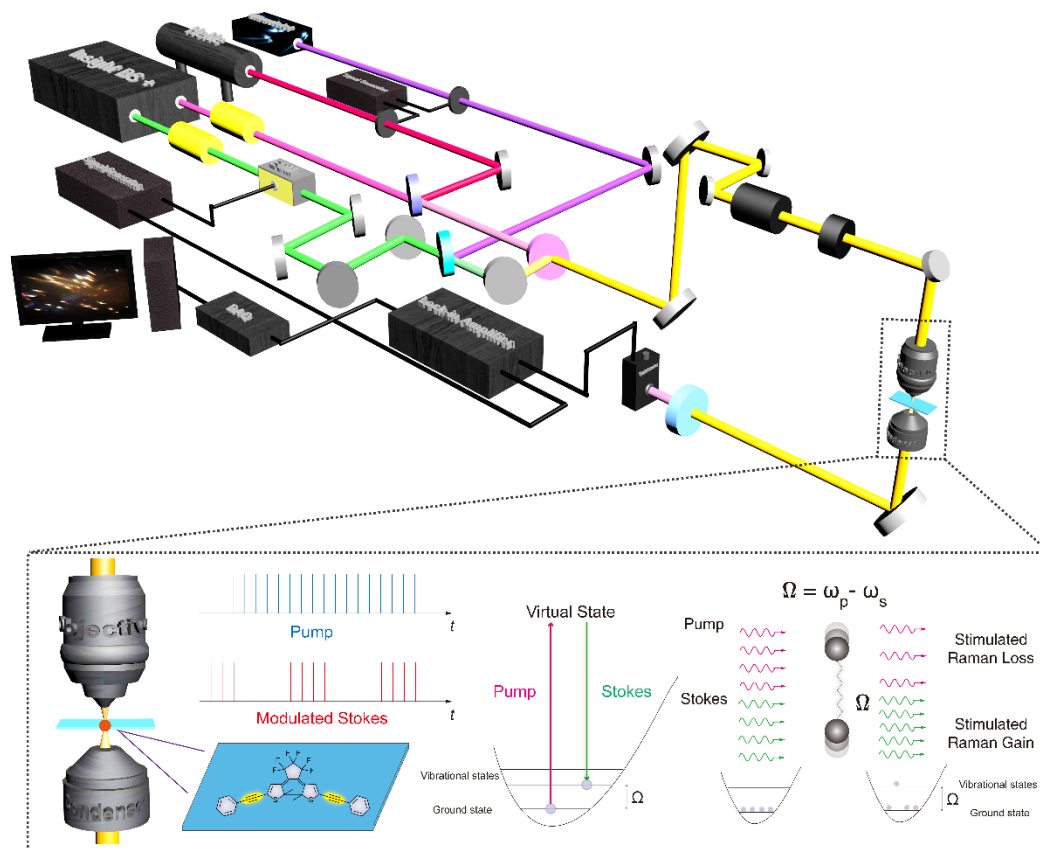
117 **Supplementary Fig. 4.** Two-photon excited photo-cycloreversion of continuous 1064

118 nm irradiation during spontaneous Raman measurements, resulting in partial photo-

119 cyclization after UV irradiation.

120

121

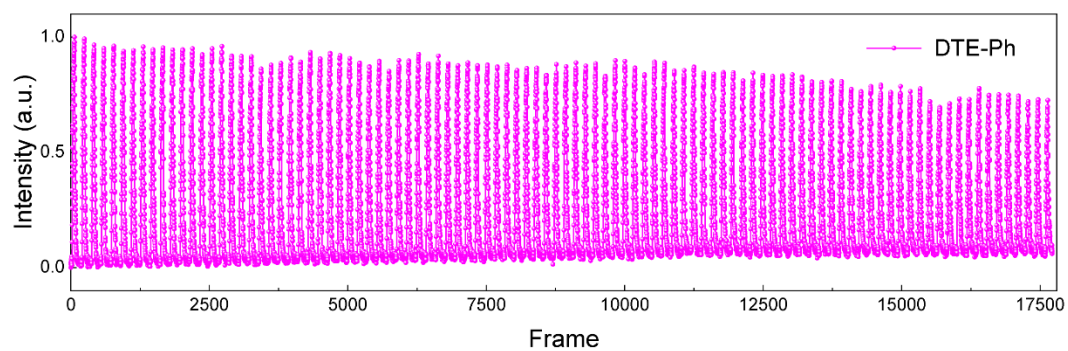


122

123 **Supplementary Fig. 5.** Optical layout of the experimental apparatus.

124

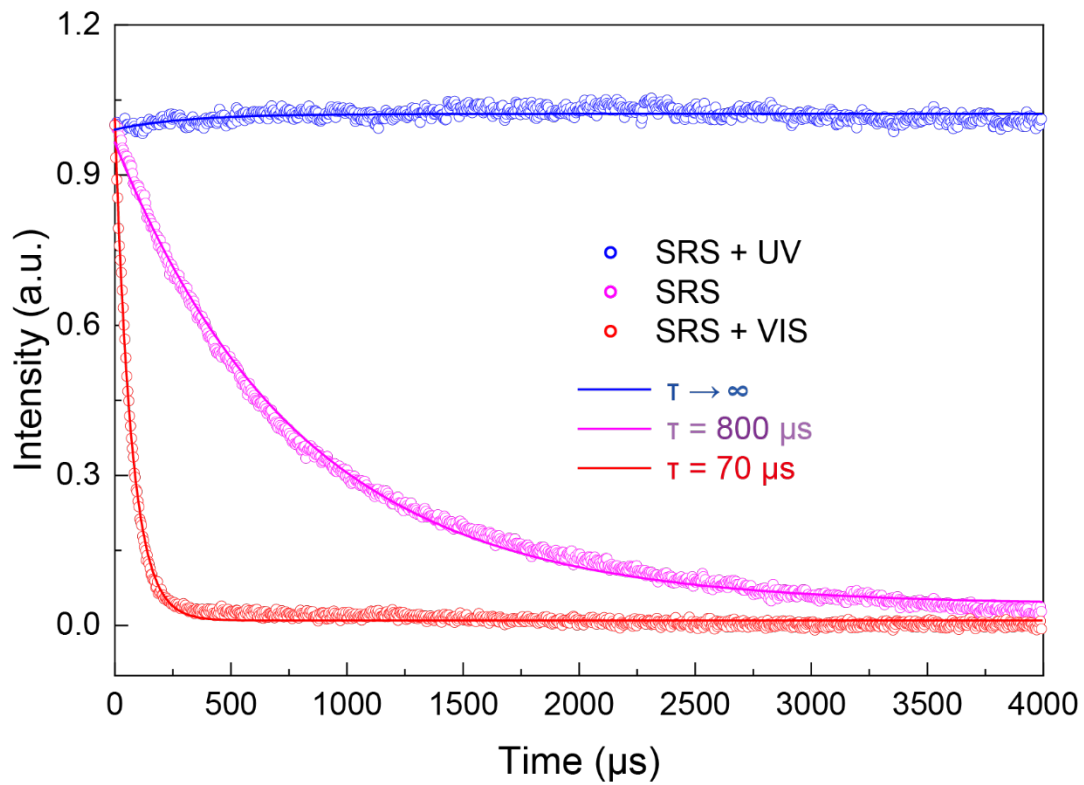
125



126

127 **Supplementary Fig. 6.** The fatigue feature of DTE-Ph, representing 100 full
128 conversion cycles (over 17500 frames, 28 ms/frame, 16×12 pixels).

129



130

131 **Supplementary Fig. 7.** Stability characterization of the photoactive Raman peak (2194

132 cm^{-1}) under different excitation conditions during SRS imaging. With normal SRS

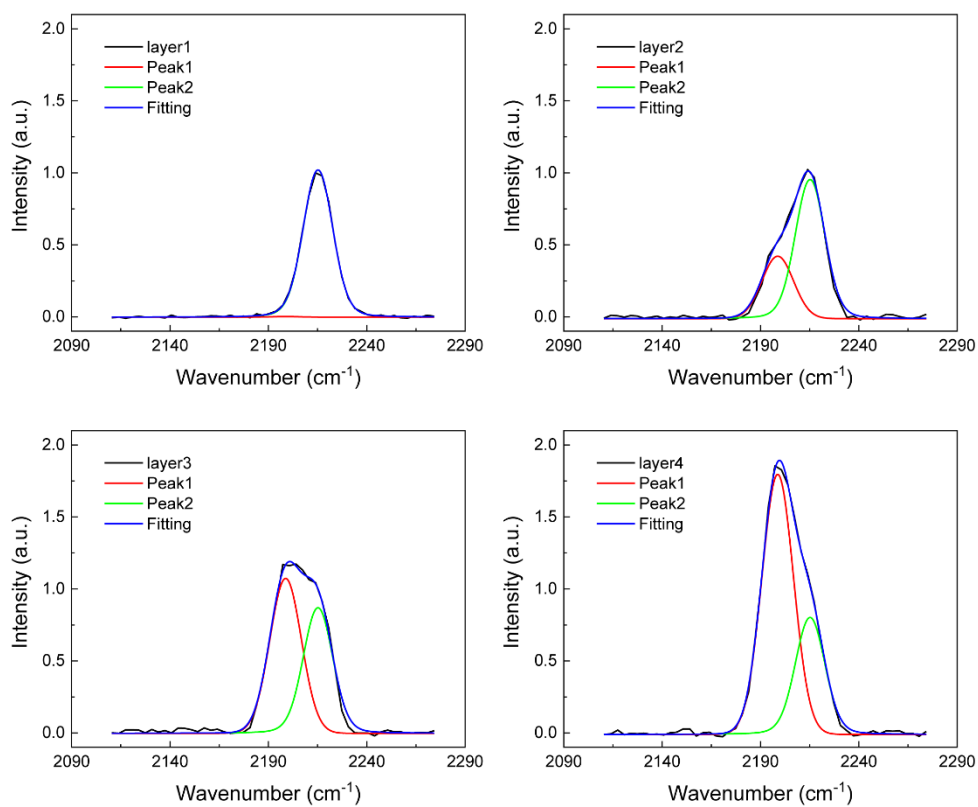
133 condition, only the pump and Stokes beams interact with the sample, the SRS signal

134 shows a slow decay after ~ 400 image frames ($2 \mu\text{s}/\text{pixel}$). With an additional visible

135 beam, the SRS signal is quenched ~ 10 times faster. Whereas with UV beam, the SRS

136 signal stays almost persistent.

137



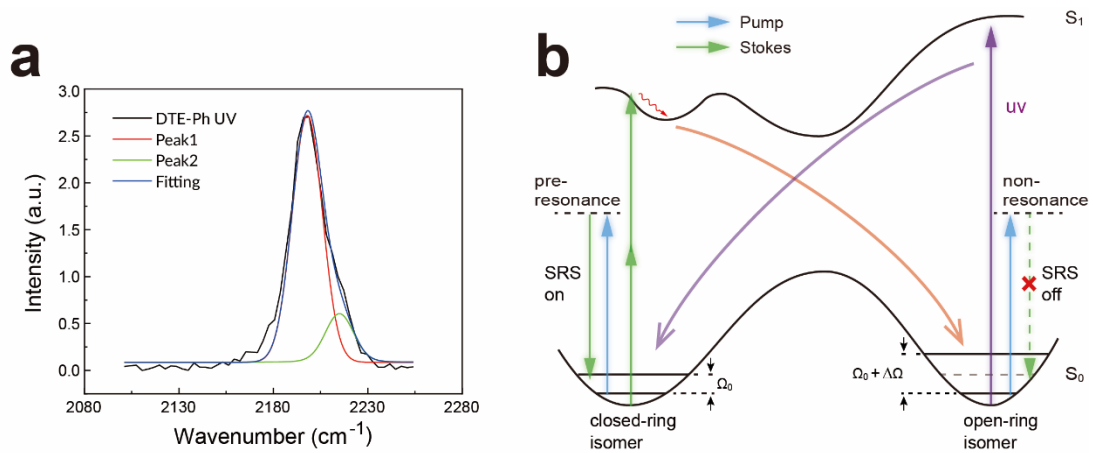
138

139 **Supplementary Fig. 8.** Spectral decomposition analysis of the SRS spectra of DTE-Ph

140 PMMA film under different UV irradiation time (Layer 1: 0 μs ; Layer 2: 50 μs ; Layer

141 3: 100 μs ; Layer 4: 150 μs).

142



143

144 **Supplementary Fig. 9.** The equilibrium between continuous UV and pump, Stokes

145 irradiation. (a) Spectral decomposition analysis of the SRS spectra of DTE-Ph in Fig.

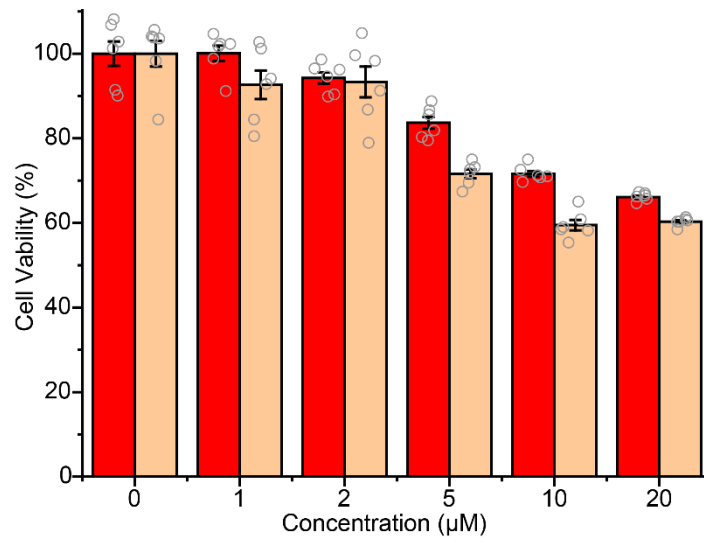
146 1c. (b) Schematic diagram of the equilibrium between UV photo-cyclization and SRS

147 two-photon induced photo-cycloreversion.

148

149

150

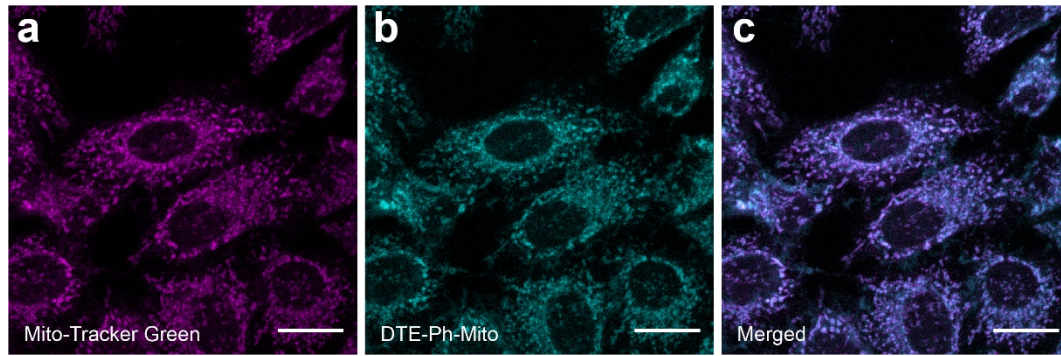


151

152 **Supplementary Fig. 10.** Cell viability tested by MTT assay of DTE-Ph-Mito cultured

153 HeLa cells (n=6 biologically independent samples, data shown as mean \pm SD).

154



155

156

157

158

159

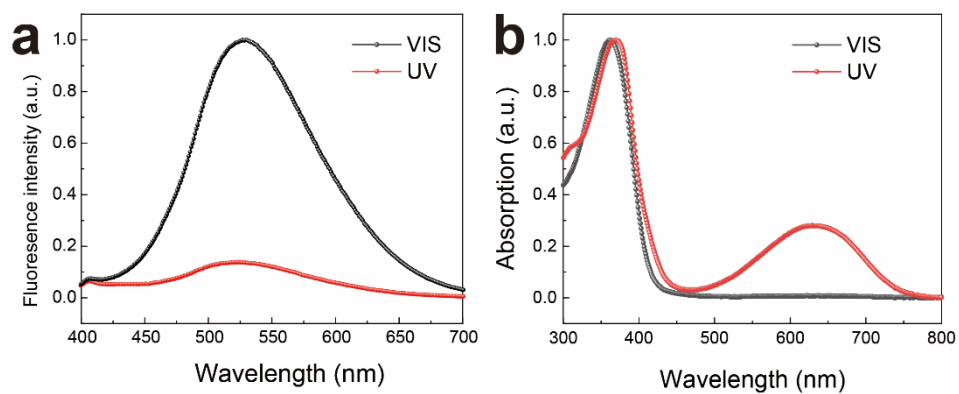
160

161

162

163

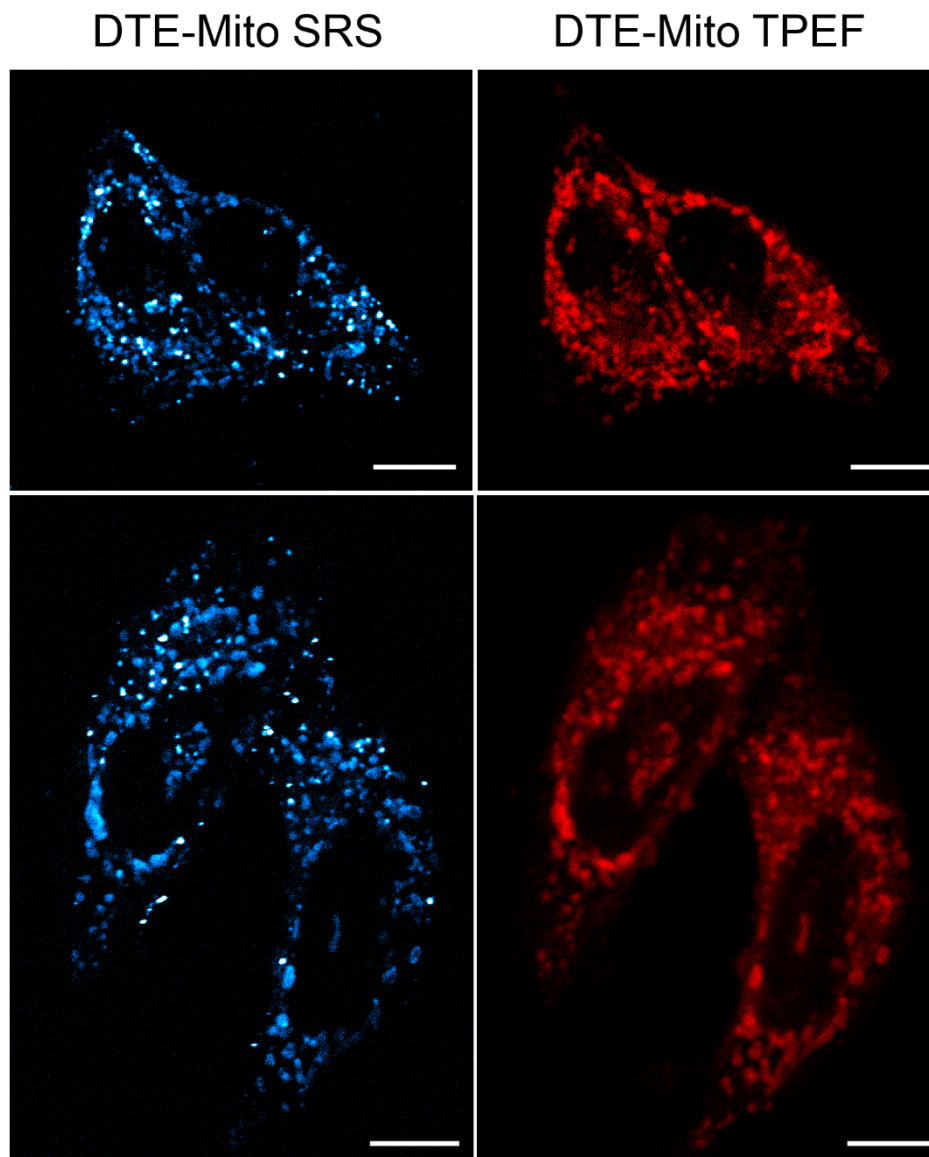
Supplementary Fig. 11. Mitochondrial labeling specificity of DTE-Ph-Mito. Two-photon fluorescent images of HeLa cells co-stained with (a) Mito-Tracker Green (50 nM) and (b) DTE-Ph-Mito (4 μ M) in culture medium for 20 min. (c) Merged image of (a) and (b). Excitation wavelength 976 nm for Mito-Tracker Green and 801 nm for DTE-Ph-Mito. Scale bar: 20 μ m.



165

166 **Supplementary Fig. 12.** Photophysical properties of DTE-Ph-Mito. (a) The
167 fluorescence (excitation wavelength: 362 nm) and (b) absorption spectra of DTE-Ph-
168 Mito after UV and visible irradiations.

169

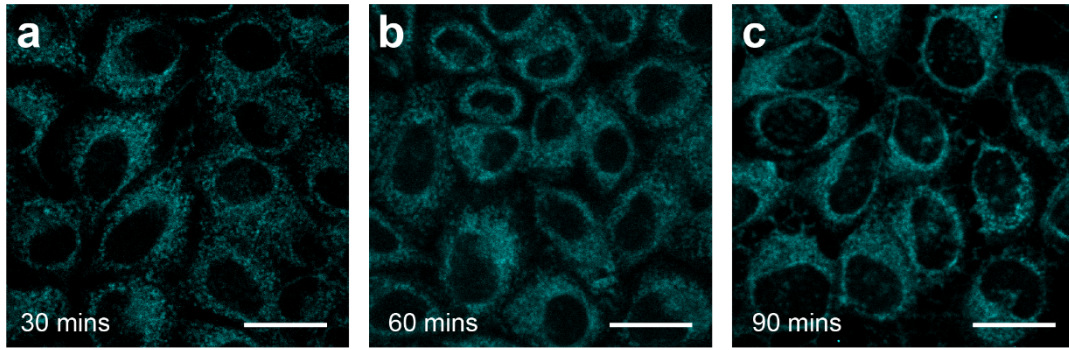


170

171 **Supplementary Fig. 13.** Co-localization images of DTE-Ph-Mito with SRS and TPEF.

172 Scale bar: 10 μ m.

173



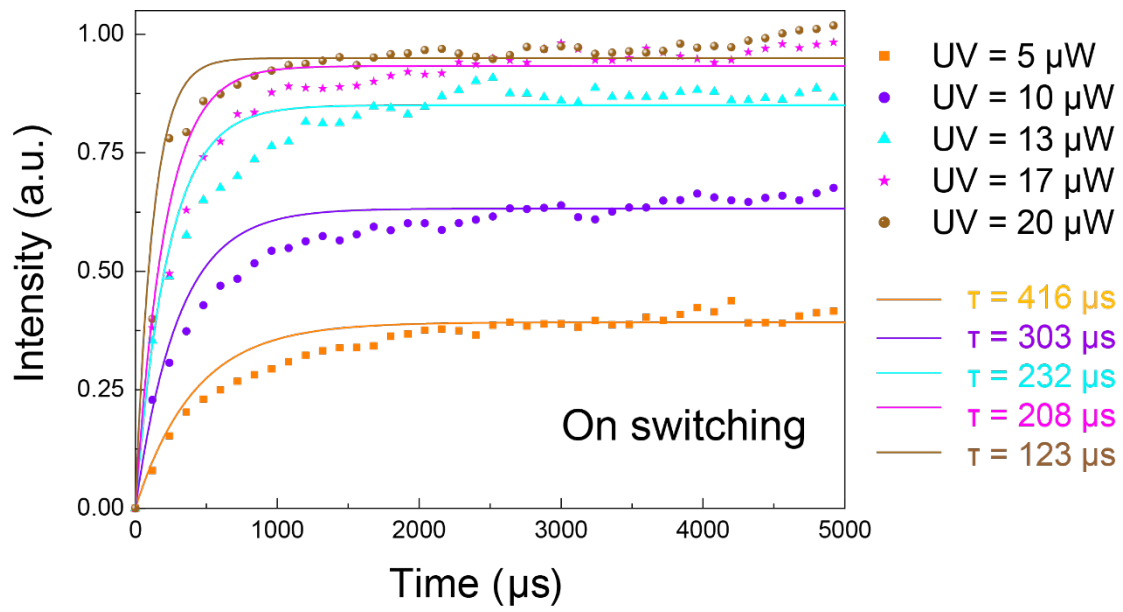
174

175 **Supplementary Fig. 14.** Fluorescence images of HeLa cells stained with 10 μ M DTE-

176 Ph-Mito for (A) 30 mins, (B) 60 mins, and (C) 90 mins. Scale bar: 20 μ m.

177

178



179

180 **Supplementary Fig. 15.** Transition dynamics of SRS intensity triggered by UV pulses.

181

182

183

184

185

Supplementary Table 1. Decomposition analysis of the four-layered SRS spectra in Figure 2a.

	closed	open	efficiency	amplification ratio
Layer 4	1.8036	0.8033	0.2084	8.6441
Layer 3	1.0738	0.8634	0.1366	7.8586
Layer 2	0.4235	0.9464	0.0536	7.9026
Layer 1	0	1	0	NA

186

187

188 **Reference**

- 189 1 Fraysse, S., Coudret, C. & Launay, J.-P. Synthesis and Properties of Dinuclear Complexes
190 with a Photochromic Bridge: An Intervalence Electron Transfer Switching “On” and
191 “Off” . *Eur. J. Inorg. Chem.* **2000**, 1581-1590, doi:10.1002/1099-
192 0682(200007)2000:7<1581::Aid-ejic1581>3.0.Co;2-2 (2000).
- 193 2 Osuka, A., Fujikane, D., Shinmori, H., Kobatake, S. & Irie, M. Synthesis and
194 photoisomerization of dithienylethene-bridged diporphyrins. *J. Org. Chem.* **66**, 3913-
195 3923, doi:10.1021/jo010001p (2001).
- 196 3 Ma, J. *et al.* Photoswitching of the triplet excited state of diiodobodipy-dithienylethene
197 triads and application in photo-controllable triplet-triplet annihilation upconversion. *J.*
198 *Org. Chem.* **79**, 10855-10866, doi:10.1021/jo5018662 (2014).
- 199 4 Buchwald, T. *et al.* Identifying compositional and structural changes in spongy and
200 subchondral bone from the hip joints of patients with osteoarthritis using Raman
201 spectroscopy. *J. Biomed. Opt.* **17**, 017007, doi:10.1117/1.JBO.17.1.017007 (2012).

202